

**Short thesis for the degree of doctor of philosophy  
(PhD)**

**Synthesis, physico-chemical, radiochemical  
and preclinical characterization of  
radiopharmaceuticals based on metal  
complexes**

by Dániel Szűcs

Supervisors:

Dr. Anikó Fekete

Prof. Imre Tóth



UNIVERSITY OF DEBRECEN

Doctoral School of Chemistry

Debrecen, 2025

# 1 Introduction and objectives

Positron emission tomography (PET) and single photon emission computed tomography (SPECT) are advanced functional imaging techniques that enable the quantitative investigation of metabolic and biochemical processes in tissues under in vivo conditions. The essence of the method is that a biologically active molecule labeled with a radioactive isotope is introduced into the living organism, and by detecting the emitted radioactivity, we can gain insight into the physiological processes taking place in the organism. PET technique is particularly important in oncological diagnostics, since the increased glucose metabolism of malignant cells can be well detected with the radiopharmaceutical 2- $^{18}\text{F}$ fluoro-2-deoxy-glucose ( $^{18}\text{F}$ FDG).

Hypoxia in tumor tissues is a state of oxygen deficiency that occurs due to inadequate blood supply to rapidly growing tumors. The resulting hypoxic microclimate has a significant impact on tumor biology, malignancy, and reduces the effectiveness of anticancer therapies. At the cellular level, oxygen deficiency leads to

the activation of hypoxia-induced factors (HIFs). These transcription factors trigger gene expression changes that promote angiogenesis and increase cell survival in a hypoxic environment. Hypoxia also increases tumor aggressiveness and metastatic potential and reduces the effectiveness of radiation therapy and certain chemotherapy agents. Early detection of oxygen-deficient areas of the tumor can be an important aid in the planning of chemo- and radiation therapies.

**One of the topics of my research work was the synthesis, physicochemical, radiochemical and preclinical investigation of  $^{44}\text{Sc}$ - and  $^{52}\text{Mn}$ -labeled radiopharmaceuticals containing a 2-nitroimidazole moiety suitable for the detection of tumor hypoxia by PET imaging.**

The increasing popularity of targeted radiotherapy has significantly increased the interest in innovative radiopharmaceutical platforms that simultaneously provide stable radiometal binding, high in vivo stability, and conjugation to biologically relevant molecules. Polyoxometalates (POMs), especially polyoxopalladates (POPs), are excellent candidates for radiometal delivery

due to their well-defined, charge-controlled structures and metal ion binding capacity. Bi-POP complexes coordinating bismuth ions synthesized by Kortz et al. offer new opportunities for targeted radiotherapy drug development.

**In this topic, the aim of our research was to create POP systems containing radioactive bismuth isotopes. By using appropriate capping groups – azide and carboxyl functionalized phenyl-arsenate units – allows the conjugation of Bi-POP complexes to biomolecules for selective tumor targeting.**

Since access to the clinically relevant,  $\alpha$ -emitting bismuth-213 isotope is limited, therefore, a  $\gamma$ -emitting bismuth-205/206 isotope mixture was used as a surrogate for radiochemical studies. Bismuth-205/206 isotopes are suitable for evaluating the formation, stability and radioisotope binding ability of the complexes due to their identical chemical behavior.

Melanoma is one of the skin tumors with the worst prognosis, which originates from pigment-producing melanocytes and, due to its increased metastatic potential, can metastasize to lymph nodes and distant organs in a

short time. Early diagnosis and in vivo detection of metastases are crucial for survival. Molecular imaging methods, including PET and SPECT, offer the possibility of targeted detection of melanoma with selective radiopharmaceuticals.

The melanocortin-1 receptor (MC1R) is highly expressed on the surface of melanoma cells, making it a suitable target for the development of diagnostic and therapeutic radioligands. NAPamide is a small peptide that binds to MC1R with high affinity, therefore, its derivatives promising candidates for melanoma-selective imaging and therapy. However, due to its small size, NAPamide is rapidly eliminated from the body, which limits its accumulation in tumor tissues and thus impairs its use as a radiopharmaceutical. One known method for increasing the circulation time of peptides is conjugation to a molecule that binds to albumin, such as 4-(p-iodophenyl)butanoic acid (IPB).

**The third topic of my research was the preparation of a NAPamide derivative modified with an albumin binding unit (IPB). After radiolabeling, it becomes suitable for the in vivo detection of melanoma and/or**

**potentially for therapy, depending on the nuclear properties of the radiometal used.**

The synthesized compound was labeled with gallium-68, bismuth-205/206, and lutetium-177 isotopes, and then the diagnostic and therapeutic applicability of the radiocomplexes was evaluated by *in vivo* and *ex vivo* biodistribution studies.

## **2 Methods used**

Analytical grade reagents were used for the syntheses, while ultra-pure chemicals were used for radioactive labeling.

Column chromatography purification of the PC2AM<sup>nBu</sup> ligand was performed on a CombiFlash® EZ Prep compact flash chromatograph equipped with a UV-VIS detector, using a Redisep® Rf Gold silica gel flash column. Reaction monitoring and product purity were performed on a Waters 2690 Separation Module analytical HPLC system equipped with a Waters 996 diode array detector and a Phenomenex Luna® 5 µm C18(2) 100 Å, 150 x 4.6 column. The final purification of the ligand was performed using a YL9100 HPLC system (Youngin

Chromass) coupled with a YL9120S UV/VIS detector, and the separation was performed on a Phenomenex Luna® 5 µm C18(2) 100 Å, 250 x 21.2 mm column.

The <sup>1</sup>H- and <sup>13</sup>C-NMR spectra of the compounds were recorded with Bruker Avance DRX 360 MHz, Bruker DRX-400 MHz and Bruker Avance II 500 spectrometers. The HR-MS spectra were measured with a Bruker maXis II UHR ESI-QTOF MS instrument at the Department of Inorganic and Analytical Chemistry of the University of Debrecen.

During the preparation of the DO3AM-NI ligand, a Kieselgel 60 F254 (Merck) TLC plate was applied for thin layer chromatography, while the compounds were detected by UV light. LC-MS measurements were performed using a maXis II UHR ESI-QTOF MS Bruker mass spectrometer connected to a Waters Acquity UPLC Iclass system. The Waters LC Module 1 HPLC system with a Luna C18 10 µm (250 x 10 mm) column was used for semi-preparative HPLC purifications. For analytical HPLC studies, a Waters 2695 Alliance HPLC system with a Luna C18 3 µm (150 x 4.6 mm) column was applied. In the case of the semi-preparative HPLC system, a UV

detector was used, while in the case of radioanalytical measurements, an ATOMKI 120 CsI scintillation radioactive detector was used in addition to the UV detector. For the radiochemical experiments, the gallium-68 isotope was obtained from a  $^{68}\text{Ge}/^{68}\text{Ga}$  isotope generator (Eckert-Ziegler), but for some experiments, the  $^{68}\text{Ga}$  isotope produced in the cyclotron at the Department of Nuclear Medicine of the University of Debrecen was applied. The other isotopes used, scandium-44, manganese-52 and bismuth-205/206, were also produced in the cyclotron at the above-mentioned department. The lutetium-177 isotope was purchased from IZINTA Trading Co. Ltd. The radioactivity of the samples was determined on a CAPINTEC CRC-15PET device. The radioactivity on the iTLC chromatograms was detected with a MiniGinta TLC scanner and the data were evaluated with the GINA-Star TLC software. The radioactivity of the biological samples was measured with a Perkin-Elmer Packard 406 Cobra gamma counter. PET images were taken with the miniPET II and miniPET III cameras.

### 3 New scientific results

**3.1 We determined the stability constant of the Sc(DO3AM-NI) complex ( $\log K_{ScL} = 22.36(4)$ ), which was significantly smaller than that of the DOTA and DTPA complexes. However, the rate of acid-catalyzed dissociation of the Sc(DO3AM-NI) complex is a quarter of that of Sc(DOTA), which indicates an exceptionally high inertness.**

For our studies, we used the DO3AM-NI ligand known from literature (Figure 1.).

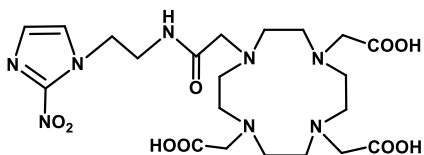


**Figure 1.** Structure of the DO3AM-NI ligand

The measurements were performed in the pH range 1.72 and 11.85 (37 °C I = 0.15 M NaCl), based on which five protonation steps were determined. The basicity of the ligand is lower ( $\log \beta_{015} = 25.10$ ) than that of the DOTA ligand ( $\log \beta_{015} = 33.68$ ). The stability constant of the Sc(DO3AM-NI) complex was determined by  $^1\text{H}$  and  $^{45}\text{Sc}$ -

NMR studies. Its thermodynamic stability constant ( $\log K_{\text{ScL}} = 22.36(4)$ ) is significantly lower than the values determined for the DOTA and DTPA ligands. Since the comparison of basicity can be misleading when comparing different ligands, we compared pSc values that are more representative of the stability ( $\text{pSc}_{(\text{DO3M-NI})} = 20.74$ ,  $\text{pSc}_{(\text{DOTA})} = 23.92$ ,  $\text{pSc}_{(\text{DTPA})} = 23.88$ ), showing smaller difference. In the case of macrocycles, acid-catalyzed dissociation is the main dissociation pathway, so we investigated the rate of dissociation of the complex in the presence of a strong acid (1 M HCl). Parallel experiments were performed, and the following rate constants were obtained:  $(1.55 \pm 0.04) \times 10^{-6} \text{ s}^{-1}$  and  $(1.67 \pm 0.05) \times 10^{-6} \text{ s}^{-1}$  (Figure 2.). The value obtained for Sc(DO3AM-NI) is one-fourth of the rate constant determined for the Sc(DOTA) complex under the same conditions.

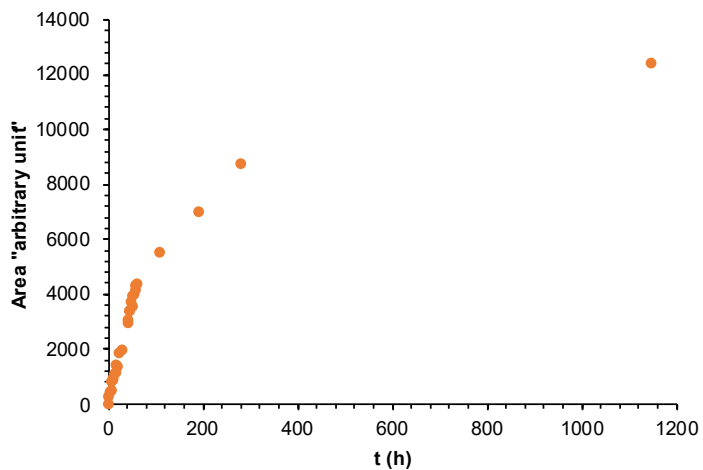


**Figure 2.**  $^{45}\text{Sc}$  NMR peak area corresponding to free Sc(III) as a function of time during the dissociation of Sc-DO3AM-NI in 1.0 M HCl ( $C_{\text{complex}} = 7.30 \text{ mM}$ ;  $I = 1.0 \text{ M}$ ;  $25 \text{ }^\circ\text{C}$ ).

**3.2 DO3AM-NI ligand was labeled with the positron-emitting scandium-44 isotope. The radiocomplex was purified and tested using various stability methods, which showed that its radiochemical purity exceeded 98% even after 4 hours under the tested conditions. We determined the octanol-water partition coefficient of [<sup>44</sup>Sc]Sc-DO3AM-NI (logP = -3.89), which indicated that the complex is hydrophilic.**

The scandium-44 isotope used for radiolabeling was prepared in a cyclotron by irradiation of natural calcium. The scandium-44 isotope was purified from the target material and possible other metal contaminants. Then, the following reaction mixture was prepared: 5  $\mu$ L of DO3AM-NI stock solution (1 mg/mL) was added to 500  $\mu$ L of [<sup>44</sup>Sc]ScCl<sub>3</sub> (100-150 MBq in 0,1 M HCl), 100  $\mu$ L of NaOAc/HOAc buffer (3 M, pH = 4), and 20  $\mu$ L of 5% NaOH, then was heated at 95°C for 15 minutes. The resulting radiocomplex was purified by solid phase extraction (SPE), and the LiChrolute EN column was found to be the most suitable for this purpose. The

radiochemical purity of the compound was determined by radio-HPLC (Figure 3.).

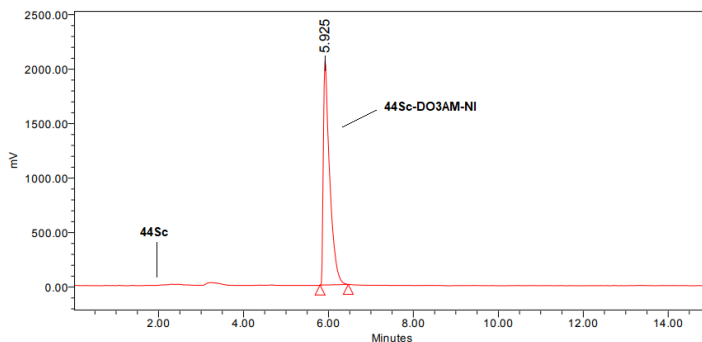


**Figure 3.** Radiochromatogram of purified [ $^{44}\text{Sc}$ ]Sc-DO3AM-NI. A Luna C18 3  $\mu\text{m}$  (150 x 4.6 mm) column was used for radio-HPLC analysis. Solvent A was oxalic acid (0.01 M pH = 3); solvent B was acetonitrile.

The [ $^{68}\text{Ga}$ ]Ga-DO3AM-NI complex known from the literature was also prepared as a reference compound. The stability of both radiopharmaceuticals was investigated at room temperature in mouse plasma and in the presence of  $\text{Na}_2\text{H}_2\text{EDTA}$  and oxalic acid. Samples were taken from the mixtures at different time points and analyzed by radio-HPLC. The radiochemical purity of the complexes was still above 98 % after 240 minutes. The logP of both compounds was measured, which gave a value of -3.89 for [ $^{68}\text{Ga}$ ]Ga-DO3AM-NI and -2.59 for

[<sup>44</sup>Sc]Sc-DO3AM-NI. The low logP values indicate that both radiopharmaceuticals are hydrophilic.

**3.3 The in vivo and ex vivo biodistribution of <sup>44</sup>Sc- and <sup>68</sup>Ga-labeled radiopharmaceuticals has been determined using healthy and KB tumor-bearing mice. Both compounds are excreted via the kidneys. The scandium-44 labeled radiopharmaceutical has better imaging properties than the gallium-68 labeled radiopharmaceutical.**

First, we investigated the in vivo and ex vivo organ distribution of the radiocomplexes in healthy mice. PET/MRI images were taken 90 and 240 minutes after the administration of the radiopharmaceuticals. The PET images clearly showed high accumulation of radiocomplexes in the kidney and urinary bladder, thus we can conclude that they are excreted through the kidney. However, in the case of [<sup>68</sup>Ga]Ga-DO3AM-NI, we obtained higher standardized uptake values (SUV) in the liver, spleen, kidney, intestines, lungs, heart and brain compared to the [<sup>44</sup>Sc]Sc-DO3AM-NI. These results were

also supported by the 90- and 240-minute ex vivo organ distribution studies.

After that, PET images were taken in SCID mice with KB tumors under the above-mentioned conditions (Figure 4.).

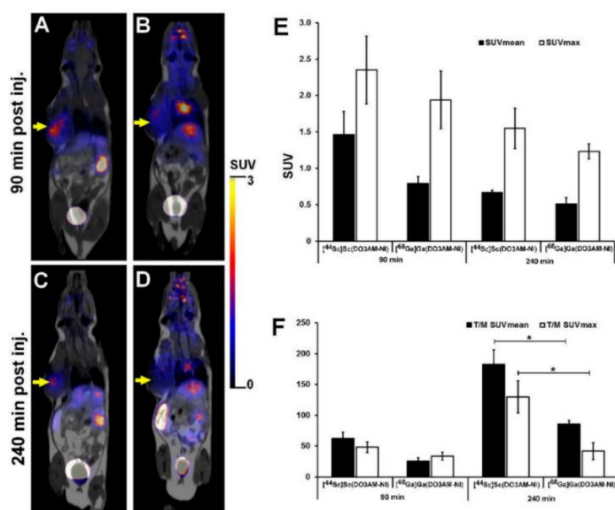


**Figure 4.** Representative in vivo whole body PET/MRI images of KB tumor-bearing mice using [<sup>44</sup>Sc]Sc-DO3AM-NI (A, C) and [<sup>68</sup>Ga]Ga-DO3AM-NI (B, D) 90 and 240 min after intravenous tracer injection. Quantitative SUV analysis of [<sup>44</sup>Sc]Sc-DO3AM-NI and [<sup>68</sup>Ga]Ga-DO3AM-NI accumulation in KB tumors (E, F). Decay-corrected PET/MRI images and data were obtained 13 ± 1 days after tumor cell inoculation. Yellow arrow: KB tumors. Significance level: p ≤ 0.01 (\*).

Based on the analysis of the PET images, the SUV<sub>mean</sub> was  $1.46 \pm 0.32$  and SUV<sub>max</sub> was  $2.35 \pm 0.47$  for [<sup>44</sup>Sc]Sc-DO3AM-NI at 90 minutes, while the SUV<sub>mean</sub> was  $0.67 \pm 0.03$  and SUV<sub>max</sub> was  $1.55 \pm 0.28$  at 240 minutes. For the <sup>68</sup>Ga-labeled molecule, the SUV<sub>mean</sub> was  $0.79 \pm 0.10$  and SUV<sub>max</sub> was  $1.94 \pm 0.40$  at 90 minutes, while the SUV<sub>mean</sub> was  $0.51 \pm 0.09$  and SUV<sub>max</sub> was  $1.23 \pm 0.10$  at 240 minutes.

In summary, there was no significant difference in the accumulation of the two radiocomplexes in KB tumors. However, a significantly higher accumulation of [<sup>68</sup>Ga]Ga(DO3AM-NI) was found in liver, spleen, kidney, intestine, lung, heart and brain than for <sup>44</sup>Sc-labeled ligand. Thus, the tumor-to-muscle (T/M) ratio of [<sup>44</sup>Sc]Sc(DO3AM-NI) was approximately 10–15-fold higher than that of [<sup>68</sup>Ga]Ga(DO3AM-NI) at all time points. This means that [<sup>44</sup>Sc]Sc(DO3AM-NI) allows the visualization of KB tumors with higher resolution, making it a promising hypoxia-specific PET radiotracer.

Furthermore, these results were correlated well with the ex vivo biodistribution studies.

**3.4 We investigated the physicochemical properties of the complexes of the PC2AM-NI and PC2A-Ph-NI ligands with Mn(II) and Sc(III) ions. PC2AM-NI is potentially suitable for binding manganese ions. The stability of Sc(PC2AM<sup>n</sup>Bu) is only one order of magnitude lower than that of Sc(PCTA), while its inertness is significantly better.**

The structures of the ligands studied during the physicochemical studies are shown in Figure 5.

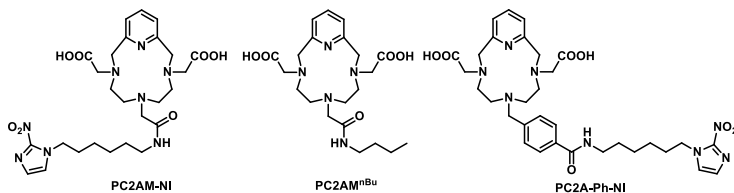


**Figure 5.** Structure of the studied ligands

The protonation constants of the PC2AM derivatives were determined by pH-potentiometry. The measured values show that the electron-withdrawing groups reduce the basicity of the amino groups of the macrocycle, thus the PC2AM ligands have lower protonation constants than the reference ligands PCTA and 3,9-PC2A.

The stability of the complexes of the PC2AM-NI ligand with Mn(II) ions was determined by potentiometric and UV-visible spectrophotometric methods. The complexes of PC2AM-NI are generally less stable than the complexes of the reference ligands, which is explained by the weaker coordination ability of the amide groups. According to the pMn values interpreted at physiological pH, the stability of the Mn(PC2AM-NI) complex is similar to that of the Mn(3,9-PC2A) complex, therefore it is potentially suitable for binding Mn(II) ions.

The stability of the complexes formed with Sc(III)-ion was investigated using  $^{45}\text{Sc}$ -NMR spectroscopy and pH-potentiometry. The measurements were performed with the model compound PC2AM<sup>nBu</sup>, which in its structure well represents the behavior of the PC2AM-NI ligand. Based on the NMR measurements, the Sc(PC2AM<sup>nBu</sup>)<sup>+</sup> complex forms a stable, deprotonation-resistant parent complex, which probably does not contain a coordinated water molecule. The stability constants were calculated using the PSEQUAD program and compared with the corresponding values for the Sc(PCTA)-complex. The results show that the introduction of the amide group

reduces the thermodynamic stability, but at the same time increases the inertness of Sc(PC2AM<sup>nBu</sup>).

**3.5 The ligands PC2AM-NI and PC2A-Ph-NI were labeled with manganese-52 and scandium-44 isotopes. The temperature and concentration dependence of the formation of manganese-52 complexes was investigated.**

The [<sup>52</sup>Mn]MnCl<sub>2</sub> solution obtained after purification of the manganese-52 isotope produced in the cyclotron was adjusted to pH = 4 with 1 M HEPES (pH = 7). Then, reaction mixtures with different ligand concentrations (0.0001, 0.001, 0.01, 0.1 and 1 mM) were prepared by adding the stock solutions of the ligands. The reaction mixtures were heated for 10 minutes at 37 and 95°C, respectively. Afterwards, samples were taken from the reactions and analyzed by radio-thin layer chromatography (radio-TLC) using iTLC-SG paper developed with mobile phase 0.5 M citrate solution (pH = 5.5). In the case of PC2AM-NI, even the lower ligand concentration was sufficient for the complete incorporation of the metal isotopes at both temperatures.

The radiolabeling of the ligands with scandium-44 were carried out as follows: 250  $\mu\text{L}$  of  $\text{NH}_4\text{OAc}/\text{HOAc}$  buffer (3M,  $\text{pH} = 4$ ) and 60  $\mu\text{L}$  of ligand stock solution (1 mg/mL) were added to 100  $\mu\text{L}$  of  $^{44}\text{Sc}]\text{ScCl}_3$  solution. The mixture was heated at  $95^\circ\text{C}$  for 15 min. The labeling yield was 95% for  $^{44}\text{Sc}]\text{Sc-PC2AM-NI}$ , while it was 96% for  $^{44}\text{Sc}]\text{Sc-PC2A-Ph-NI}$ .

The radiolabeled complexes were purified from buffer and free radiometal ions on a Sep-Pak C18 Plus Light (Waters) SPE column.

**3.6 The stability of the radiolabeled complexes was investigated in serum, in the presence of EDTA and essential metal ions. Based on this, a significant ligand exchange took place within four hours in the case of <sup>52</sup>Mn-labeled complexes, while in the presence of serum proteins and essential metal ions no transformation was observed. The <sup>44</sup>Sc-labeled complexes remained intact under the tested conditions. The logP value of the complexes was also determined, which indicate that they exhibit hydrophilic properties.**

In vitro serum stability studies of radiolabeled compounds were performed by mixing aqueous solutions of the complexes with rat serum. For ligand exchange experiments, 0.2 M EDTA (pH = 7.4) solution was used. For metal ion exchange, 0.1 mM ZnCl<sub>2</sub> (1 μL), 0.01 mM CuCl<sub>2</sub> (1 μL), 1.02 mM MgCl<sub>2</sub> (24 μL) and 2.28 mM CaCl<sub>2</sub> (24 μL) solutions were mixed and added to the aqueous solution of the radiocomplexes. The mixtures were incubated for 4 hours at room temperature. In the case of both radiopharmaceuticals, there was no transformation in serum and in the presence of metal ions.

However, in the case of ligand exchange, after 4 hours, 48% of the [ $^{52}\text{Mn}$ ]Mn-PC2AM-NI complex remained intact, while only 22% of the [ $^{52}\text{Mn}$ ]Mn-PC2A-Ph-NI complex remained stable. There was no change in the  $^{44}\text{Sc}$ -labeled compounds after 4 hours under the tested conditions. The logP values of the radiocomplexes were determined, which were -2.32 for [ $^{52}\text{Mn}$ ]Mn-PC2AM-NI and -1.42 for [ $^{52}\text{Mn}$ ]Mn-PC2A-Ph-NI. Similar values were obtained when examining the  $^{44}\text{Sc}$ -labeled complexes, since the logP was -2.44 for [ $^{44}\text{Sc}$ ]Sc-PC2AM-NI and -1.25 for [ $^{44}\text{Sc}$ ]Sc-PC2A-Ph-NI. Based on the obtained results, the radiopharmaceuticals are hydrophilic. The difference in the logP values of the complexes is likely due to the phenyl group of PC2A-Ph-NI.

**3.7 Ex vivo biodistribution experiments were used to investigate the elimination of radiopharmaceuticals from the body, which showed that excretion occurred not only through the kidneys but also through the hepatobiliary system. In the case of the [ $^{52}\text{Mn}$ ]Mn-PC2AM-NI complex, significant accumulation was measured in several non-target organs.**

For the ex vivo organ distribution study, healthy (control) C57Bl6 mice were used. The studies were performed 90 and 240 minutes after the administration of the radiopharmaceuticals. High radiotracer uptake was observed in the liver, kidneys, small and large intestines, and gallbladder at both time points for each radiocomplex. Low uptake was observed in the other abdominal and thoracic organs after 90 and 240 minutes of incubation with the  $^{44}\text{Sc}$ -labeled compounds and [ $^{52}\text{Mn}$ ]Mn-PC2A-Ph-NI. In contrast, in the case of the [ $^{52}\text{Mn}$ ]Mn-PC2AM-NI complex, relatively high accumulation was observed in the lungs, heart, salivary glands, and pancreas at both time points.

**3.8 PET images were obtained from B16F10 melanoma tumor-bearing mice, which were correlated well with the results of ex vivo studies. Based on the PET images,  $^{52}\text{Mn}$ - and  $^{44}\text{Sc}$ -labeled PC2A-Ph-NI was suitable for detecting tumor hypoxia.**

The radiopharmaceuticals were injected into the tail vein of B16F10 tumor-bearing mice, and PET images were obtained 90 and 240 minutes later (Figure 6.). Based on the analysis of the PET images, hypoxic areas of subcutaneously growing B16F10 melanoma tumors can be clearly identified with the  $^{52}\text{Mn}$ - and  $^{44}\text{Sc}$ -labeled PC2A-Ph-NI targeting hypoxic cells. In contrast, low tumor accumulation and tumor-to-muscle ratios were obtained with the  $^{52}\text{Mn}$ - and  $^{44}\text{Sc}$ -labeled PC2AM-NI complexes, so these radiolabeled compounds are not suitable for the detection of hypoxic regions of the tumor in their current form.

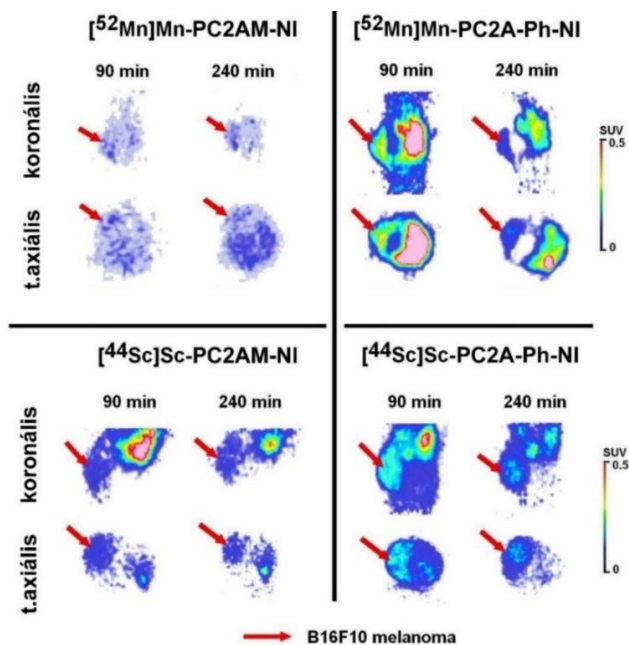


**Figure 6.** Decay-corrected PET images of B16F10 melanoma tumor-bearing mice 90 and 240 minutes after intravenous injection of  $[^{52}\text{Mn}]\text{Mn-PC2AM-NI}$ ,  $[^{52}\text{Mn}]\text{Mn-PC2A-Ph-NI}$ , and  $[^{44}\text{Sc}]\text{Sc-PC2AM-NI}$  and  $[^{44}\text{Sc}]\text{Sc-PC2A-Ph-NI}$ . Red arrows indicate B16F10 tumors.

**3.9 We successfully prepared radioactive bismuth-labeled Bi-POP complexes and developed a chromatographic method for the detection of the complexes. [<sup>205/206</sup>Bi]BiPd12AsL complex was purified by solid-phase extraction, and then a serum stability test was carried out with the purified compound.**

During the research, we successfully prepared four different radioactive Bi-POP complexes, namely [<sup>205/206</sup>Bi]BiPd12AsL, [<sup>205/206</sup>Bi]BiPd12AsLN, [<sup>205/206</sup>Bi]BiPd12AsLC and [<sup>205/206</sup>Bi]BiPd15PL. The labeling reactions were conducted in sodium acetate buffer in the presence of Pd(OAc)<sub>2</sub> at 80°C. The incorporation of radioactive bismuth was monitored by radio-TLC and iTLC methods. The developed iTLC method resulted in a smaller baseline, thereby enabling more accurate detection of the four [<sup>205/206</sup>Bi]Bi-POP complexes (Figure 7.).

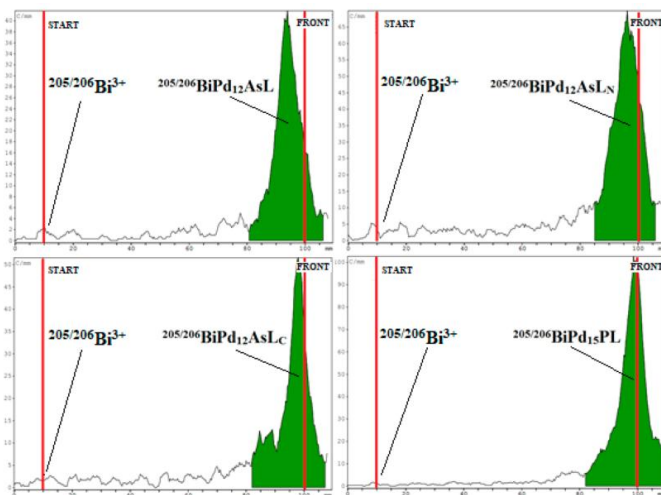


**Figure 7.** Radio-iTLC chromatograms of the  $[^{205/206}\text{Bi}]\text{BiPd}_{12}\text{AsL}$ ,  $[^{205/206}\text{Bi}]\text{BiPd}_{12}\text{AsLN}$ ,  $[^{205/206}\text{Bi}]\text{BiPd}_{12}\text{AsLC}$  and  $[^{205/206}\text{Bi}]\text{BiPd}_{15}\text{PL}$  reaction mixtures (stationary phase: iTLC-SG paper, mobile phase: 0.05 M  $\text{Na}_2\text{CO}_3$ )

The radiochemical yield was greater than 99% in all cases after 10 min of reaction. The reversed-phase TLC method was necessary for identifying radioactive complexes with non-radioactive standard Bi-POP complexes, while the iTLC method was more suitable for purity analysis.

The  $[^{205/206}\text{Bi}]\text{BiPd}_{12}\text{AsL}$  complex was purified by solid-phase extraction on a Sep-Pak C18 Plus Light (Waters) column. In the case of the other three complexes,

SPE purification was unsuccessful, either due to inadequate binding or irreversible adsorption. During in vitro stability studies, the [ $^{205/206}\text{Bi}$ ]BiPd12AsL complex showed rapid aggregation in rat serum, which could be caused by the strong interaction between the numerous aromatic capping groups in the complex and serum proteins.

During the radiochemical studies, we had the opportunity to conduct preliminary experiments with the  $^{213}\text{Bi}$  isotope and successfully prepared the [ $^{213}\text{Bi}$ ]BiPd12AsL and [ $^{213}\text{Bi}$ ]BiPd12AsL<sub>N</sub> complexes. However, the short availability of the generator limited the further experiments.

**3.10 My third research topic was the pharmacokinetic study of radiolabeled DOTA-NAPamide derivatives with an albumin-binding unit. First, we achieved the synthesis of a NAPamide derivative conjugated with 4-(p-iodophenyl)-butanoic acid and DOTA chelator.**

DOTA-IPB-NAPamide (**10**) was prepared by multi-step solid-phase peptide synthesis (Figure 8.). In the

synthesis, a protected lysine derivative (**1**) was first coupled to the resin-bound NAPamide peptide (**2**), followed by removal of the 9-fluorenylmethoxycarbonyl (Fmoc) protecting group. The resulting derivative **4** was conjugated with 4-(p-iodophenyl)butanoic acid (**5**), followed by removal of the 1-(4,4-dimethyl-2,6-dioxocyclohex-1-ylidene)ethyl (Dde) protecting group. DOTA-tris(t-Bu) ester was then coupled to the free amino group of the peptide derivative **7**. The final step of the synthesis was acidic hydrolysis with trifluoroacetic acid, which removed the protecting groups and cleaved the target compound from the resin. The crude product was purified by semi-preparative HPLC and then identified by mass spectrometry.

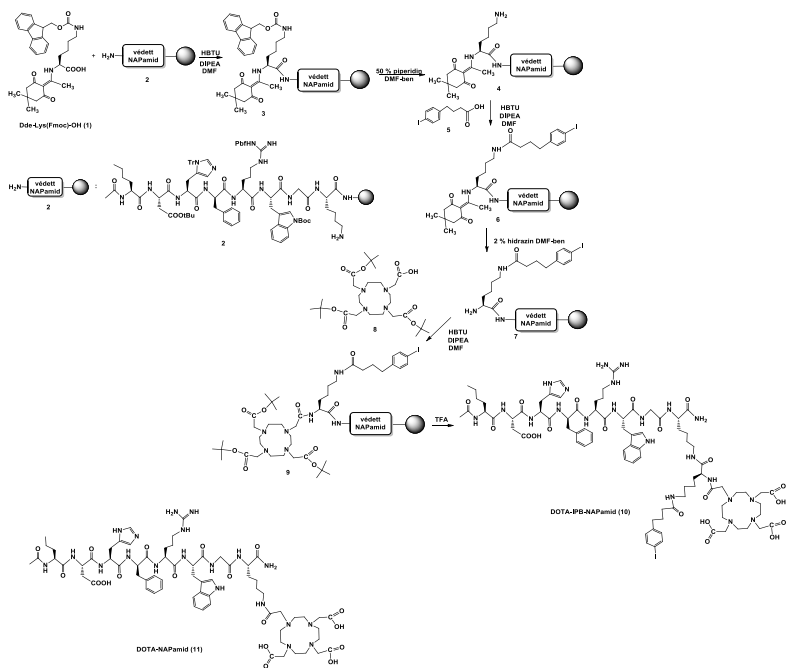


**Figure 8.** Synthesis of DOTA-IPB-NAPamide (**10**) containing an albumin binding unit

**3.11 The DOTA-IPB-NAPamide ligand was labeled with gallium-68, bismuth-205/206 and lutetium-177 isotopes and the purification of the resulting radiopharmaceuticals was achieved. The radiolabeled metal complexes were stable in serum, in the presence of EDTA and essential metal ions during the study period. The incorporation of the albumin binding moiety made the complexes more lipophilic compared to the reference compounds.**

The radiolabeling of DOTA-IPB-NAPamide was first performed with the positron-emitting  $^{68}\text{Ga}$  isotope, which was prepared in a cyclotron and used after several steps of purification. The reaction was carried out at  $95^{\circ}\text{C}$  in the presence of  $\text{NH}_4\text{OAc}/\text{HOAc}$  buffer, and the resulting radiocomplex was purified by solid-phase extraction on a Sep-Pak C18 Plus Light (Waters) column. The yield of labeling was  $>98\%$ . For preclinical studies, the ligand was also successfully complexed with the isotope mixture bismuth-205/206 – which served as an alternative to the alpha-emitting bismuth-213 – and with the beta-emitting [ $^{177}\text{Lu}$ ]lutetium ion. In all cases,

excellent labeling yields of  $\geq 98\%$  and radiochemical purity were achieved. In addition, the commercially available DOTA-NAPamide compound was also labeled with these isotopes, and the resulting complexes were used as references in preclinical studies. The purity of the radiolabeled products was confirmed by radio-HPLC and radio-iTLC.

After purification, in vitro stability studies of the labeled compounds were performed in serum, 0.2 M EDTA solution (pH = 7.4) and in the presence of various essential metal ions ( $\text{Mg}^{2+}$ : 0.51 mM,  $\text{Ca}^{2+}$ : 1.14 mM,  $\text{Zn}^{2+}$ : 0.01 mM,  $\text{Cu}^{2+}$ : 0.001 mM). During the analysis of samples taken at different time points, no signs of decomposition of the radiocomplexes were observed, which means that these compounds are stable in serum and resistant to ligand and metal ion exchange under the conditions tested.

In addition, the logP values of the radiopharmaceuticals were determined, which are summarized in the table below. Based on the results, complexes with an albumin binding unit (IPB) showed higher lipophilicity than the reference compounds.

Table 1. logP values of DOTA-NAPamide and DOTA-IPD-NAPamide labeled with different radiometals.

	logP values of DOTA-NAPamide complexes	logP values of DOTA-IPB-NAPamide complexes
gallium-68 labeled	-3,46	-2,12
bizmut-205/206 labeled	-3,65	-2,32
lutécium-177 labeled	-2,60	-1,26

**3.12 We performed in vivo and ex vivo distribution studies of  $^{68}\text{Ga}$ -,  $^{205/206}\text{Bi}$ - and  $^{177}\text{Lu}$ -labeled complexes, based on which the introduction of the albumin binding unit (IPB) was most favorable in the case of the radiopharmaceutical labeled with the long-half-life lutetium-177 isotope.**

The tumor targeting and organ distribution of the [ $^{68}\text{Ga}$ ]Ga-DOTA-NAPamide and [ $^{68}\text{Ga}$ ]Ga-DOTA-IPB-NAPamide were investigated in mice bearing B16F10 melanoma by in vivo PET imaging (Figure 9.) and ex vivo biodistribution studies. The B16F10 tumor model, characterized by high MC1-R expression, is excellent for the preclinical evaluation of MC1-R-specific radiopharmaceuticals. Both  $^{68}\text{Ga}$ -labeled compounds

clearly detected tumors, confirming that they effectively bind to the MC1-R receptor.

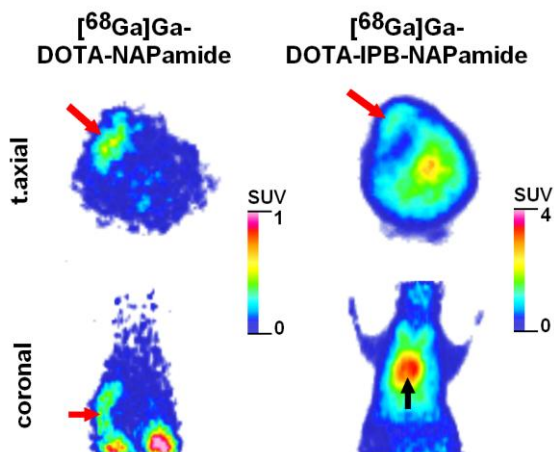


**Figure 9.** Representative decay-corrected PET images of mice bearing B16F10 melanoma tumors 90 min after intravenous injection of  $[^{68}\text{Ga}]\text{Ga-DOTA-NAPamide}$  and  $[^{68}\text{Ga}]\text{Ga-DOTA-IPB-NAPamide}$  and  $9 \pm 1$  days after transplantation of MC1-R positive mouse B16F10 melanoma cells. **Red arrows:** B16F10 tumor, **black arrow:** heart.

However, quantitative analysis of PET images showed a significant difference between the two compounds:  $[^{68}\text{Ga}]\text{Ga-DOTA-IPB-NAPamide}$  resulted in higher tumor accumulation ( $\text{SUV}_{\text{mean}} = 1.31 \pm 0.24$ ) than  $[^{68}\text{Ga}]\text{Ga-DOTA-NAPamide}$  ( $\text{SUV}_{\text{mean}} = 0.43 \pm 0.09$ ;  $p < 0.05$ ). This could be attributed to the biological effect of

the IPB-based albumin binding moiety, which slowed down the clearance of the radiopharmaceutical and thereby enhanced its accumulation in the tumor. The same phenomenon was observed in ex vivo studies. In addition, [<sup>68</sup>Ga]Ga-DOTA-IPB-NAPamide showed higher uptake in most organs ( $p \leq 0.01$ ), and the high %ID/g value measured in the blood 90 minutes after administration ( $14.21 \pm 1.87$ ) also indicated a prolonged circulation time. In contrast, [<sup>68</sup>Ga]Ga-DOTA-NAPamide showed low background accumulation except in the kidneys. The presence of the albumin binding moiety reduced the potential of the [<sup>68</sup>Ga]Ga-DOTA-IPB-NAPamide complex as a diagnostic PET agent compared to the reference compound, mainly due to the high radiopharmaceutical accumulation found in non-target organs.

To evaluate the MC1-R specificity and tissue uptake pattern of the [<sup>205/206</sup>Bi]Bi-DOTA-NAPamide and [<sup>205/206</sup>Bi]Bi-DOTA-IPB-NAPamide, we performed ex vivo biodistribution studies using B16F10 tumor-bearing mice. Significant differences in the organ distribution of the radiopharmaceuticals were observed during the study.

$[^{205/206}\text{Bi}]\text{Bi-DOTA-IPB-NAPamide}$ , which contains an albumin-binding moiety, showed higher accumulation in most organs and tissues, including liver, lung, heart, and blood, compared to  $[^{205/206}\text{Bi}]\text{Bi-DOTA-NAPamide}$ . This may be attributed to the lipophilic nature of the compound and the presence of the albumin-binding moiety, which resulted in a longer circulation time and hepatobiliary elimination. In contrast,  $[^{205/206}\text{Bi}]\text{Bi-DOTA-NAPamide}$  showed rapid renal clearance, low blood uptake, and high renal accumulation. Both compounds showed specific binding to B16F10 melanoma tumors. However,  $[^{205/206}\text{Bi}]\text{Bi-DOTA-NAPamide}$  had lower background uptake and a higher tumor/background ratio, which is more advantageous for clinical application.

In vivo SPECT/CT studies with  $[^{177}\text{Lu}]\text{Lu-DOTA-IPB-NAPamide}$  were performed. The B16F10 melanoma tumor was clearly detectable 24 hours after the administration of the radiopharmaceutical, while in the case of the reference compound without the albumin binding unit, the tumor was not detectable at all. (Figure 10.) This indicates that in the case of the  $^{177}\text{Lu}$ -labeled compound, the presence of the IPB unit significantly

improves the tumor targeting ability and retention and therapeutic efficacy of the compound.

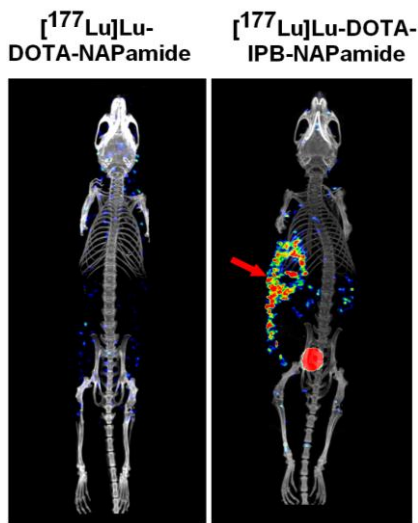


**Figure 10.** Representative MIP SPECT/CT scans of B16F10 tumor-bearing mice 24 hours after intravenous administration of  $[^{177}\text{Lu}]\text{Lu-DOTA-NAPamide}$  and  $[^{177}\text{Lu}]\text{Lu-DOTA-IPB-NAPamide}$  and  $9 \pm 1$  days after subcutaneous MC1-R positive B16F10 cell implantation. **Red arrow:** B16F10 tumor. MIP: 3D maximum intensity projection.

Ex vivo biodistribution studies also confirmed the above results, as in this study  $[^{177}\text{Lu}]\text{Lu-DOTA-IPB-NAPamide}$  also showed significantly higher tumor uptake than the reference compound without the albumin-binding moiety. However, the presence of the IPB moiety not only

increased tumor accumulation and retention, but also resulted in higher uptake in the liver, kidneys and blood-rich organs, which was also a consequence of the increased circulation time.

Based on our studies, the introduction of the albumin-binding moiety proved to be advantageous in the case of the long-half-life  $^{177}\text{Lu}$ -labeled radiopharmaceutical, as it resulted in significant tumor uptake and retention, so that this compound can exert its therapeutic effect even 24 hours after administration. In contrast, in the case of the shorter-half-life  $^{68}\text{Ga}$ - and  $^{205/206}\text{Bi}$ -labeled compounds, the increased circulation time caused by the IPB moiety increased tumor accumulation, but also resulted in significant background uptake, which degrades the quality of imaging and causes significant radiation exposure in non-target organs. The use of a weaker albumin-binding moiety, such as p-(tolyl)butyric acid, instead of IPB, can eliminate this problem.

## 4 Possibilities for the utilization of the results

Preclinical studies of [ $^{44}\text{Sc}$ ]Sc-DO3AM-NI have shown that this radiopharmaceutical has better imaging properties in detecting tumor hypoxia than the reference [ $^{68}\text{Ga}$ ]Ga-DO3AM-NI. In addition, the longer half-life of the  $^{44}\text{Sc}$  isotope makes it suitable for transport and use in distant PET centers. Compared to the currently used  $^{18}\text{F}$ -FMISO in the clinic, this molecule is much more hydrophilic, so it does not accumulate in the brain, but its faster elimination results in a higher contrast PET image.

PC2AM-NI ligand can be considered as a good Mn(II)-binding chelator, since complex formation is complete above pH = 4. The complex is inert towards acid-catalyzed dissociation. The moderate relaxivity of Mn(PC2AM-NI) indicates the absence of a water molecule coordinating to the metal ion, therefore it cannot be used as an MRI contrast agent but can be used in PET imaging. Furthermore, the stability of Sc(PC2AM<sup>nBu</sup>) (model compound of PC2A-Ph-NI) is only one order of magnitude lower than that of Sc(PCTA), while its

inertness is significantly better, which is an important parameter in the case of radiopharmaceuticals used in PET imaging.

The **PC2AM-NI** and **PC2A-Ph-NI** ligands were labeled with positron-emitting isotopes scandium-44 and manganese-52, and the resulting radiopharmaceuticals were studied by in vivo PET imaging and ex vivo distribution studies, which showed that the  $^{44}\text{Sc}$  and  $^{52}\text{Mn}$ -labeled **PC2A-Ph-NI** ligand are suitable for detecting hypoxic regions of the tumor.

Among the four POP complexes ( $^{205/206}\text{Bi}|\text{BiPd12AsL}$ ,  $^{205/206}\text{Bi}|\text{BiPd12AsLN}$ ,  $^{205/206}\text{Bi}|\text{BiPd12AsLC}$  and  $^{205/206}\text{Bi}|\text{BiPd15PL}$ ) prepared by us, the  $^{205/206}\text{Bi}|\text{BiPd12AsL}$  and  $^{205/206}\text{Bi}|\text{BiPd12AsLN}$  complexes containing conjugable azide and carboxyl groups are of biological significance. Namely, these POP complexes can be linked to biologically relevant molecules, which makes them suitable for targeted radionuclide therapy. The labeling took place in 10 minutes with high efficiency, which is advantageous for the short half-life, alpha-therapeutic bismuth-213 isotope.

The radiolabeled **DOTA-IPB-NAPamide** complexes had an increased circulation time due to the IPB albumin-binding unit. This was not advantageous in the case of complexes labeled with short half-live isotopes ( $^{68}\text{Ga}$ ,  $^{213}\text{Bi}$ ), because although it increased the accumulation of radiopharmaceuticals in melanoma tumors, it also caused high radiopharmaceutical uptake values in blood-reach organs compared to the compound without the albumin-binding unit. However, during the preclinical study of the complexes labeled with the long-half-live  $^{177}\text{Lu}$  isotope, we found that the compound without the albumin-binding unit was not detectable in the tumor 24 hours after the administration of the radiopharmaceutical, while at this time point the tumor could be clearly detected with the **[ $^{177}\text{Lu}$ ]Lu-DOTA-IPB-NAPamide** molecule, so this radiopharmaceutical was still able to exert its therapeutic effect. Based on our research, it can be stated that the albumin binding moiety improves the tumor uptake and retention of small peptide-based,  $^{177}\text{Lu}$ -labeled radiopharmaceuticals, but for clinical use, a weaker albumin binding moiety is required instead of 4-(p-

iodophenyl)butanoic acid to reduce the radiotracer uptake in non-target organs.



Registry number: DEENK/477/2025.PL  
Subject: PhD Publication List

Candidate: Dániel Szűcs  
Doctoral School: Doctoral School of Chemistry  
MTMT ID: 10070673

### List of publications related to the dissertation

#### Foreign language scientific articles in international journals (3)

1. **Szűcs, D.**, Péli-Szabó, J., Arató, V. Z., Gyuricza, B., Szikra, D. P., Tóth, I., Képes, Z., Trencsényi, G., Fekete, A.: Investigation of the Effect on the Albumin Binding Moiety for the Pharmacokinetic Properties of 68Ga-, 205/206Bi-, and 177Lu-Labeled NAPamide-Based Radiopharmaceuticals.  
*Pharmaceuticals (Basel)*. 16 (9), 1-17, 2023. EISSN: 1424-8247.  
DOI: <http://dx.doi.org/10.3390/ph16091280>  
IF: 4.3
2. **Szűcs, D.**, Csupász, T., Péli-Szabó, J., Kis, A., Gyuricza, B., Arató, V. Z., Forgács, V., Vágner, A., Nagy, G., Garai, I., Szikra, D. P., Tóth, I., Trencsényi, G., Tircsó, G., Fekete, A.: Synthesis, physicochemical, labeling and in vivo characterization of a DO3AM-based hypoxia sensitive 44Sc-labeled PET probe.  
*Pharmaceuticals (Basel)*. 15 (6), 1-16, 2022. EISSN: 1424-8247.  
DOI: <https://doi.org/10.3390/ph15060666>  
IF: 4.6
3. Manna, P., **Szűcs, D.**, Csupász, T., Fekete, A., Szikra, D. P., Lin, Z., Gáspár, A., Bhattacharya, S., Zulaica, A., Tóth, I., Kortz, U.: Shape and Size Tuning of Billi-Centered Polyoxopalladates: High Resolution 209Bi NMR and 205/206Bi Radiolabeling for Potential Pharmaceutical Applications.  
*Inorg. Chem.* 59 (23), 16769-16782, 2020. ISSN: 0020-1669.  
DOI: <http://dx.doi.org/10.1021/acs.inorgchem.0c02857>  
IF: 5.165





### List of other publications

#### Foreign language scientific articles in international journals (11)

4. Bunda, S., Kálmán-Szabó, I., Szikra, D. P., Fekete, A., **Szűcs, D.**, Péli-Szabó, J., Trencsényi, G., Képes, Z., Kálmán, F. K.: In vivo Evaluation of Copper-61-Labeled Prostate-specific Membrane Antigen Targeting Novel Radiopharmaceutical: first Steps toward Clinical Implementation.  
*ACS Pharmacol. Transl. Sci.* 8 (6), 1580-1590, 2025. ISSN: 2575-9108.  
DOI: <http://dx.doi.org/10.1021/acspstsci.4c00685>  
IF: 3.7 (2024)
5. Bunda, S., Kálmán-Szabó, I., Lihí, N., Képes, Z., Szikra, D. P., Péli-Szabó, J., Timári, I., **Szűcs, D.**, May, N. V., Papp, G., Trencsényi, G., Kálmán, F. K.: Diagnosis of Melanoma with 61Cu-Labeled PET Tracer.  
*J. Med. Chem.* 67 (11), 9342-9354, 2024. ISSN: 0022-2623.  
DOI: <http://dx.doi.org/10.1021/acs.jmedchem.4c00479>  
IF: 6.8
6. Kálmán-Szabó, I., Bunda, S., Lihí, N., Szaniszló, Z., Szikra, D. P., Péli-Szabó, J., Fekete, A., Gyuricza, B., **Szűcs, D.**, Papp, G., Trencsényi, G., Kálmán, F. K.: 61Cu-Labeled radiodiagnostics of melanoma with NAPamide-targeted radiopharmaceutical.  
*Int. J. Pharm.* 632, 1-9, 2023. ISSN: 0378-5173.  
DOI: <http://dx.doi.org/10.1016/j.ijpharm.2022.122527>  
IF: 5.3
7. Kálmán-Szabó, I., Képes, Z., Fekete, A., Vágner, A., Nagy, G., **Szűcs, D.**, Gyuricza, B., Arató, V. Z., Varga, J., Kárpáti, L., Garai, I., Mándity, I. M., Bruchertseifer, F., Elek, J., Szikra, D. P., Trencsényi, G.: In Vivo evaluation of newly synthesized 213Bi-conjugated alpha-melanocyte stimulating hormone ( $\alpha$ -MSH) peptide analogues in melanocortin-1 receptor (MC1-R) positive experimental melanoma model.  
*J. Pharm. Biomed. Anal.* 229, 1-9, 2023. ISSN: 0731-7085.  
DOI: <http://dx.doi.org/10.1016/j.jpba.2023.115374>  
IF: 3.1
8. Lucio-Martínez, F., Esteban-Gómez, D., Laura, V., Horváth, D., **Szűcs, D.**, Fekete, A., Szikra, D. P., Tircsó, G., Platas-Iglesias, C.: Rigid H4OCTAPA derivatives as model chelators for the development of Bi(III)-based radiopharmaceuticals.  
*Chem. Commun.* 59 (23), 3443-3446, 2023. ISSN: 1359-7345.  
DOI: <http://dx.doi.org/10.1039/D2CC06876A>  
IF: 4.3





9. Képes, Z., Arató, V. Z., Péli-Szabó, J., Gyuricza, B., **Szűcs, D.**, Hajdu, I., Fekete, A., Bruchertseifer, F., Szikra, D. P., Trencsényi, G.: Therapeutic Performance Evaluation of <sup>213</sup>Bi-Labelled Aminopeptidase N (APN/CD13)-Affine NGR-Motif ([<sup>213</sup>Bi]Bi-DOTAGA-cKNGRE) in Experimental Tumour Model: a Treasured Tailor for Oncology. *Pharmaceutics*. 15 (2), 1-15, 2023. EISSN: 1999-4923.  
DOI: <http://dx.doi.org/10.3390/pharmaceutics15020491>  
IF: 4.9
10. Csupász, T., **Szűcs, D.**, Kálmán, F. K., Hollóczki, O., Fekete, A., Szikra, D. P., Tóth, É., Tóth, I., Tircsó, G.: A New Oxygen Containing Pycen-Type Ligand as a Manganese(II) Binder for MRI and <sup>52</sup>Mn PET Applications: Equilibrium, Kinetic, Relaxometric, Structural and Radiochemical Studies. *Molecules*. 27, 1-27, 2022. ISSN: 1420-3049.  
DOI: <https://doi.org/10.3390/molecules27020371>  
IF: 4.6
11. Forgács, V., Fekete, A., Gyuricza, B., **Szűcs, D.**, Trencsényi, G., Szikra, D. P.: Methods for the Determination of Transition Metal Impurities in Cyclotron-Produced Radiometals. *Pharmaceutics (Basel)*. 15 (2), 1-24, 2022. EISSN: 1424-8247.  
DOI: <https://doi.org/10.3390/ph15020147>  
IF: 4.6
12. Gyuricza, B., Szűcs, Á., Péli-Szabó, J., Arató, V. Z., Képes, Z., **Szűcs, D.**, Szikra, D. P., Trencsényi, G., Fekete, A.: The Synthesis and Preclinical Investigation of Lactosamine-Based Radiopharmaceuticals for the Detection of Galectin-3-Expressing Melanoma Cells. *Pharmaceutics*. 14, 1-16, 2022. EISSN: 1999-4923.  
DOI: <http://dx.doi.org/10.3390/pharmaceutics14112504>  
IF: 5.4
13. Gyuricza, B., Péli-Szabó, J., Arató, V. Z., Dénes, N., Szűcs, Á., Berta, K., Kis, A., **Szűcs, D.**, Forgács, V., Szikra, D. P., Kertész, I., Trencsényi, G., Fekete, A.: Synthesis of <sup>68</sup>Ga-Labelled cNGR-Based Glycopeptides and In Vivo Evaluation by PET Imaging. *Pharmaceutics*. 13 (12), 1-14, 2021. EISSN: 1999-4923.  
DOI: <http://dx.doi.org/10.3390/pharmaceutics13122103>  
IF: 6.525
14. Gyuricza, B., Péli-Szabó, J., Arató, V. Z., **Szűcs, D.**, Vágner, A., Szikra, D. P., **Fekete, A.**: Synthesis of Novel, Dual-Targeting <sup>68</sup>Ga-NODAGA-LacN-E[c(RGDfK)]<sub>2</sub> Glycopeptide as a PET Imaging Agent for Cancer Diagnosis. *Pharmaceutics*. 13 (6), 1-13, 2021. EISSN: 1999-4923.  
DOI: <http://dx.doi.org/10.3390/pharmaceutics13060796>  
IF: 6.525





Hungarian abstracts (8)

15. Farkasinszky, G., **Szűcs, D.**, Szikra, D. P., Miklovicz, T., Pótári, N., Forgács, V., Józszai, I., Trencsényi, G., Balkay, L.: A [13N] ammónia vizsgálati gyógyszer dokumentációjának (IMPD) előkészítése.  
In: Hevesy György Magyar Orvostudományi Nukleáris Társaság XXIII. Kongresszusa: Tudományos program és előadás összefoglalók, [n.a.], Visegrád, 12, 2025.
16. **Szűcs, D.**, Péli-Szabó, J., Arató, V. Z., Gyuricza, B., Szikra, D. P., Trencsényi, G., Tóth, I., Fekete, A.: 68Ga és 205/206Bi jelzett, albuminkötő egységgel módosított DOTA-konjugált NAPamid szintézise és preklinikai vizsgálata.  
In: Őszi Radiokémiai napok 2022. Szerk.: Józszai István, Magyar Kémikusok Egyesülete, Budapest, 57-60, 2022. ISBN: 9786156018137
17. Gyuricza, B., Szűcs, Á., Péli-Szabó, J., Arató, V. Z., **Szűcs, D.**, Szikra, D. P., Trencsényi, G., Fekete, A.: 68ga izotóppal jelölt, (2-naftil)-metilezett laktózamin alapú radiofarmakonok előállítására és biológiai vizsgálata.  
In: Vegyészkonferencia 2022. Szerk.: Keglevich György, Kurtán Tibor, Magyar Kémikusok Egyesülete, Eszterházy Károly Katolikus Egyetem, 82, 2022. ISBN: 9786156018113
18. **Szűcs, D.**, Péli-Szabó, J., Arató, V. Z., Gyuricza, B., Szikra, D. P., Trencsényi, G., Tóth, I., Fekete, A.: Albuminkötő egység beépítésének hatása 68Ga és 205/206Bi jelzett NAPamid alapú radiofarmakonok farmakokinetikai tulajdonságaira.  
In: 55. Komplexkémiai Kollokvium : Előadás-összefoglalók, MKE Komplexkémiai Szakcsoport, Debrecen, E18, 2022.
19. Gyuricza, B., Szűcs, Á., Péli-Szabó, J., Arató, V. Z., **Szűcs, D.**, Szikra, D. P., Trencsényi, G., Fekete, A.: Galektin-3 receptor detektálása melanoma sejtekben 68Ga-jelzett (2-naftil) metilezett laktóz-amin alapú radioligandokkal.  
In: 55. Komplexkémiai Kollokvium : Előadás-összefoglalók, MKE Komplexkémiai Szakcsoport, Debrecen, E23, 2022.
20. Gyuricza, B., Szűcs, Á., Péli-Szabó, J., Arató, V. Z., **Szűcs, D.**, Szikra, D. P., Trencsényi, G., Fekete, A.: Melanoma kimutatása PET képalkotással laktózamin-alapú Gal-3 radioligandok segítségével.  
In: Őszi Radiokémiai napok 2022. Szerk.: Józszai István, Magyar Kémikusok Egyesülete, Budapest, 102-103, 2022. ISBN: 9786156018137
21. Gyuricza, B., Péli-Szabó, J., Arató, V. Z., **Szűcs, D.**, Vágner, A., Szikra, D. P., Fekete, A.: 68Ga jelzett kettős targetálású glikopeptid alapú radiofarmakonok szintézise.  
In: Őszi Radiokémiai napok 2021. Szerk.: Józszai István, Magyar Kémikusok Egyesülete, Budapest, 39-44, 2021. ISBN: 9786156018076





22. Gyuricza, B., Péli-Szabó, J., Arató, V. Z., **Szűcs, D.**, Vágner, A., Szikra, D. P., Fekete, A.: 68GA-NODAGA-LACN-E[C(RGDFK)]<sub>2</sub> glikopeptid alapú radiofarmakon szintézise.

In: II. Fiatal Kémikusok Fóruma Szimpózium Absztraktfüzet. Szerk.: Bodor Zsanett, Ádám Adél, Bana Péter, Hegedűs Marica, Simon Fruzsina ; ill. Ziegenheim Szilveszter, MKE Fiatal Kémikusok Fóruma, S. I., 45, 2021.

**Total IF of journals (all publications): 69,815**

**Total IF of journals (publications related to the dissertation): 14,065**

The Candidate's publication data submitted to the Tudóstér have been validated by DEENK on the basis of the Journal Citation Report (Impact Factor) database.

19 August, 2025

